

Experimental Demonstration of Multi-User Full-Duplex RO-ISAC System

Shuhang Chen

School of Microelectronics and
Communication Engineering
Chongqing University
Chongqing, China
202312021097t@stu.cqu.edu.cn

Zhihong Zeng

School of Microelectronics and
Communication Engineering
Chongqing University
Chongqing, China
zhihong.zeng@cqu.edu.cn

Chen Chen

School of Microelectronics and
Communication Engineering
Chongqing University
Chongqing, China
c.chen@cqu.edu.cn

Abstract—A multi-user full-duplex retroreflective optical ISAC (RO-ISAC) system using wavelength division duplexing (WDD) and interference cancellation is proposed. Experimental results demonstrate the feasibility of multi-user joint sensing and communication in the RO-ISAC system.

Keywords—retroreflective optical integrated sensing and communication (RO-ISAC), full-duplex, multi-user

I. INTRODUCTION

The sixth-generation (6G) mobile communication systems are anticipated to simultaneously deliver high-capacity communication and high-precision sensing services to support emerging applications, including the Internet of Things, intelligent transportation systems, human-computer interactions, and environmental monitoring. As a pivotal enabling technology for 6G, integrated sensing and communication (ISAC) has garnered extensive research attention in recent years [1]. Typically, ISAC systems can be deployed utilizing either radio-frequency (RF) or optical spectrum [2]. In comparison with RF-based ISAC, optical ISAC is capable of fully leveraging the vast bandwidth inherent to light, thereby achieving both large transmission capacity and high sensing accuracy [3]. Given that optical ISAC systems typically depend on light reflected by targets to accomplish passive sensing, the notion of retroreflective optical ISAC (RO-ISAC) has been further put forward in relevant literature [4], [5]. This design incorporates a corner cube reflector (CCR) into the target to strengthen light reflection efficiency [6]. The implementation of RO-ISAC systems faces a few challenges, including bidirectional transmission, multi-user interference, etc. In our previous work, we have proposed single-user retroreflective optical ISAC (RO-ISAC) systems to achieve bidirectional transmission and sensing [7]-[9]. A practical RO-ISAC system usually needs to support multi-user bidirectional transmission between the transceiver and receivers. Due to bidirectional transmission, there might be interference between the reflected downlink signals and the uplink signals in a multi-user RO-ISAC system.

Aiming at address the multi-user full-duplex transmission and sensing, we propose a multi-user full-duplex RO-ISAC system. In addition, OFDMA is adopted in the downlink, and subcarriers are interleaved to overcome low-pass frequency responses, while DFT-S-OFDM is employed to avoid interference between users in the uplink. Experiments are conducted to study the performance of the proposed multi-user full-duplex RO-ISAC system.

II. PRINCIPLE

Fig. 1 depicts the schematic diagram of the proposed multi-user full-duplex RO-ISAC system. The system consists of a transceiver and several receivers. At the RO-ISAC transceiver, the input bits are first modulated into a real-valued OFDM signal via OFDM modulation. The obtained resultant digital OFDM signal is then converted into an analog OFDM signal via digital-to-analog (D/A) conversion and a direct current (DC) bias is added to ensure the non-negativity of the OFDM signal. Finally, the resultant downlink OFDM signal is used to drive a laser diode (LD) to generate the red light for downlink transmission. At the RO-ISAC receivers, the OFDM signals are detected by photo-detector (PDs) and analog-to-digital (A/D) conversion is then conducted to obtain a digital OFDM signal. After time synchronization, OFDM demodulation is executed to get their own output bits.

As shown in Fig. 1, the RO-ISAC receivers are equipped with CCRs respectively to reflect the red light back to realize ranging at the RO-ISAC transceiver. The inset in the RO-ISAC receiver 1 illustrates the diagram of the CCR, where L_s , L , and D_r denote the recessed length, the length, and the diameter of the CCR, respectively. Moreover, at the RO-ISAC receivers, the uplink input bits are respectively modulated into a digital DFT-S-OFDM signal. After D/A conversion and DC bias addition, the obtained DFT-S-OFDM signal is used to drive a green LED (GLED) to generate the green light for uplink transmission. After free-space transmission, the reflected red light and the green light are mixed together and a pair of optical filters are used to separate the red and green lights at the RO-ISAC transceiver to avoid the bidirectional interference. Particularly, a red optical filter (ROF) is adopted to filter out the red light from the mixed light for further ranging procedures, while a green optical filter (GOF) is applied to filter out the green light from the mixed light for uplink demodulation. After red filtering, the filtered red light is detected by a PD and the resultant analog OFDM signal is converted into a digital OFDM signal via A/D conversion. Subsequently, time-domain cross-correlation between the reflected OFDM signal and the upsampled downlink OFDM signal is performed to calculate the time of flight and hence estimate the distance. The maximum likelihood estimation of the time of flight can be represented by

$$\hat{\tau} = \arg \max_{\tau} \sum_{n=0}^{L_w-1} y(n)x(n-\tau) \quad (1)$$

where $x(n)$ and $y(n)$ respectively denote the upsampled time-domain samples of the original OFDM signal and the time-domain samples of the reflected OFDM signal, and L_w is the length of the selected time-domain window for cross-correlation. Hence, the distance d between the transceiver and

This work was supported by the National Natural Science Foundation of China under Grant 62501088, Grant 62271091 and Grant 62271093.

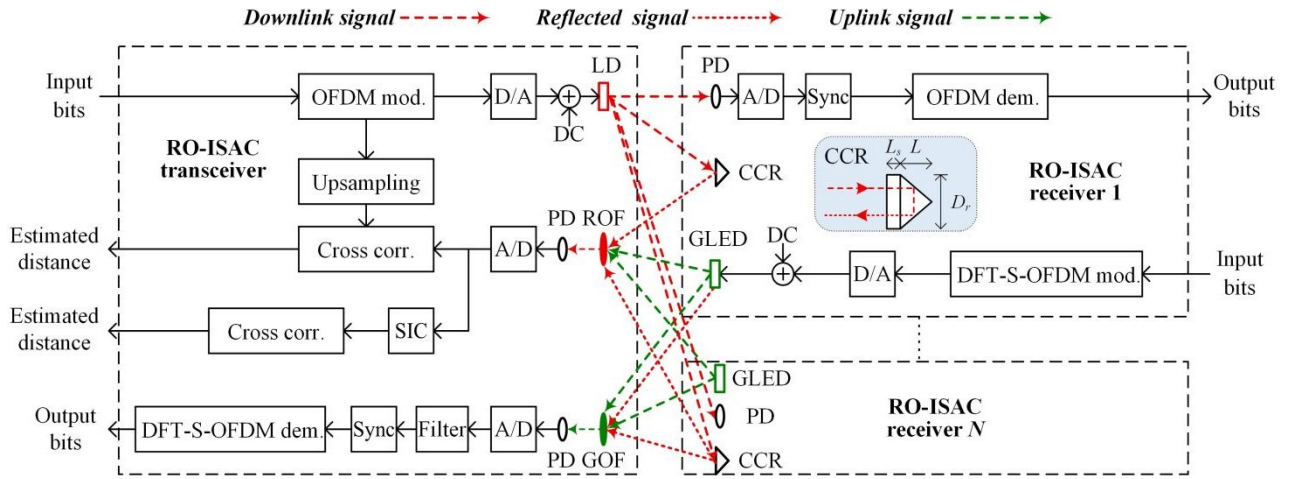


Fig. 1. Schematic diagram of the proposed multi-user full-duplex RO-ISAC system.

receiver 1 can be estimated as $\hat{d} = c\hat{\tau} / 2$ with c being the speed of light. For an A/D sampling rate f_s , the ranging resolution is given by $r=c/2f_s$. But, the filtered red light covers the reflected signal from all users. To address this challenge, we introduce an interference cancellation method. In a multi-user scenario, the reflected signals from far users will be overwhelmed by those from near users. As a result, there will be a significant peak shift when performing cross-correlation calculations on the signals of far users. To extract the signals of far users from the mixed reflected signals, it is necessary to perform interference cancellation on the mixture. As noted previously, by calculation the time-of-flight of the nearest user, we can isolate and eliminate their reflected signal from the composite set of reflected signals through the following method. First, the nearest user channel is described by

$$\hat{H} = \frac{Signal_r}{Signal_i} \quad (2)$$

where $Signal_i$ and $Signal_r$ respectively denote the transmitting OFDM signal and the received OFDM signal of nearest user. Thus, the second nearest signal is described by

$$Signal_{fr} = Signal_r - \hat{H}Signal_i \quad (3)$$

Following the aforesaid operation, we can acquire the composite reflected signal with the strongest component excluded. Next, we can utilize $Signal_{fr}$ to perform a cross-correlation computation as per Eq. (1), thereby estimating the time-of-flight for the second nearest user. By repeating this process iteratively, we can obtain the TOF values for all users and further calculate the distances between each user and the RO-ISAC transceiver.

III. EXPERIMENTAL RESULT

Fig. 2 depicts the experimental setup of the full-duplex RO-ISAC system, where a laser diodes (LD, HL63603TG) is employed in the downlink while two GLEDs are applied in the uplink. Both the downlink OFDM signal and two channels of uplink DFT-S-OFDM signals are generated offline using MATLAB, which are then loaded into three ports of two two-channel arbitrary waveform generators (AWG, Tektronix AFG31102) with sampling rates of 250, 25 and 25 MSa/s, respectively. The output OFDM signal is used to drive the LD with a DC bias voltage of 2.5 V, while two channels of output DFT-S-OFDM signals are respectively combined with a DC bias voltage of 2.7 V via a bias tee (Bias-T, Mini-Circuits ZFBT-6GW+) and then utilized to drive two GLEDs. The peak-to-peak voltage (V_{pp}) of the downlink OFDM signal is

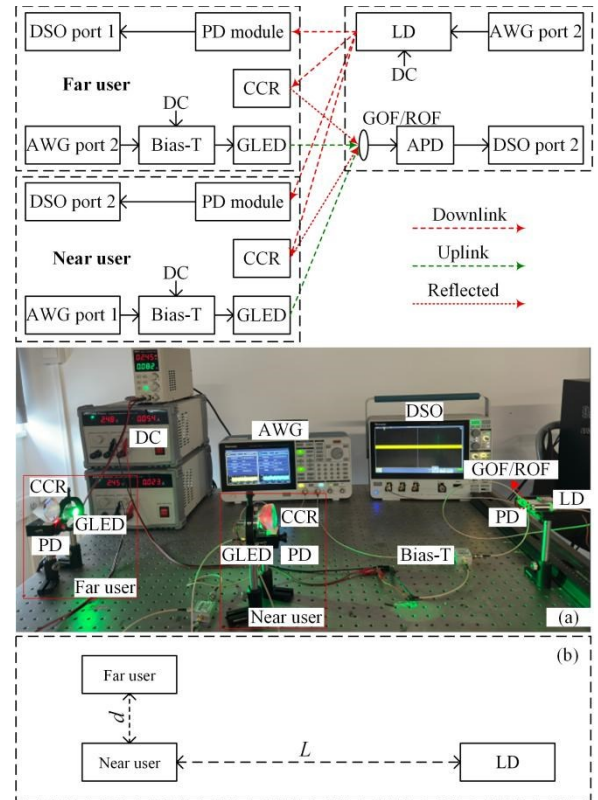


Fig. 2. Experimental setup of the two-user full-duplex RO-ISAC system.

fixed at 100 mV, while the V_{pp} of the two uplink DFT-S-OFDM signals are fixed at 850 mV respectively. In the downlink, two PD modules (HCCLS2021MOD01-RX) are used to detect the red light and the obtained OFDM signals are recorded by a digital storage oscilloscope (DSO, LeCroy Wavesurfer432) with a sampling rate of 2.5 GSa/s for downlink demodulation. In the uplink, a GOF and a ROF are respectively adopted to filter the mixed light, and an avalanche photo-diode (APD, Hamamatsu C12702-12) is used to detect the filtered optical signal. The ROF filters out the reflected red light and the detected OFDM signal is recorded by the DSO with a sampling rates of 2.5 GSa/s for ranging, while GOF filters out the green light and the detected DFT-S-OFDM signal is recorded by the DSO with a sampling rates of 250 MSa/s for uplink demodulation. The photo of the experimental testbed is shown in Fig. 2.

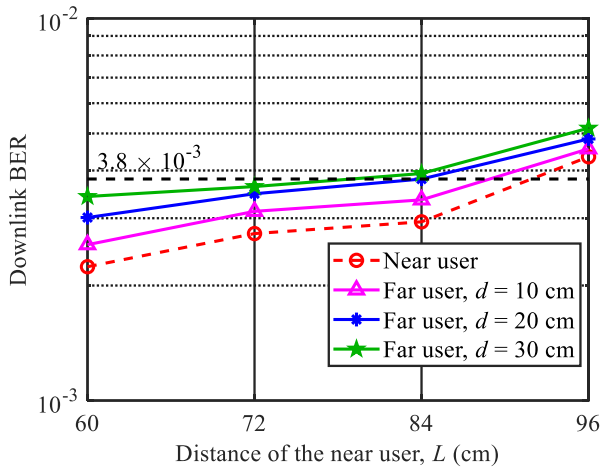


Fig. 3. Downlink BER vs. the distance of near user for different users.

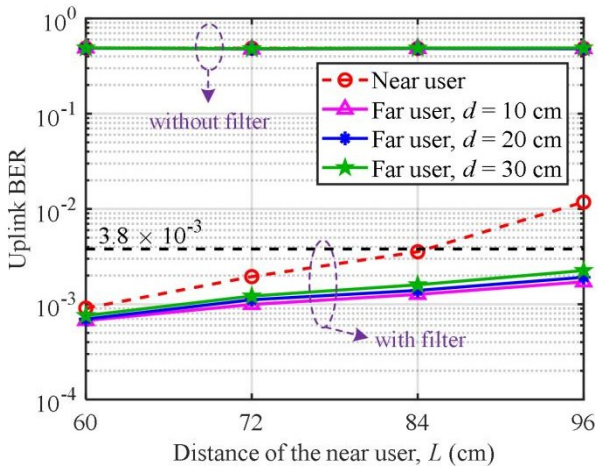


Fig. 4. Uplink BER vs. the distance of near user for different users without and with filter.

In the downlink OFDM modulation, the inverse fast Fourier transform (IFFT) size is 256 and a total of 64 subcarriers are used to carry 8-QAM (i.e., $M_{QAM} = 8$) symbols in OFDM, which is corresponding to a frequency-domain upsampling rate of $R_f = 8$. As a result, the total data rate of downlink transmission is given by $\log_2 8 \times (250/4) = 250$ Mb/s, the two user bisect the spectrum source which means the two both use 32 subcarriers to transmit their own message. We allocate 1st to 32th subcarriers to near user and 33th to 64th subcarriers to far user, and each user has the communication rate of 125 Mbit/s. In addition, a clipping ratio of 11 dB is considered during OFDM modulation in downlink transmissions. In the uplink DFT-S-OFDM modulation, the IFFT size, the number of data subcarriers and the QAM order are 256, 60 and 4, respectively. Hence, the data rate of uplink transmission is given by $\log_2 4 \times (250/(256/60)) = 11.7$ Mb/s. In addition, the far user occupies a lower-frequency subcarrier block, while the near user occupies a higher-frequency subcarrier block. For the uplink ranging, the A/D sampling rate is $f_s = 2.5$ GSa/s and hence the ranging resolution is calculated by $r = 6$ cm. Moreover, the length of time-domain window for cross-correlation calculation is set to 2650 during uplink ranging. In addition, more experimental details are shown in Fig. 2(b), L represents the horizontal distance between the near user and LD, and d represents the vertical distance between the near user and the far user. We first evaluate the communication of the full-duplex RO-ISAC

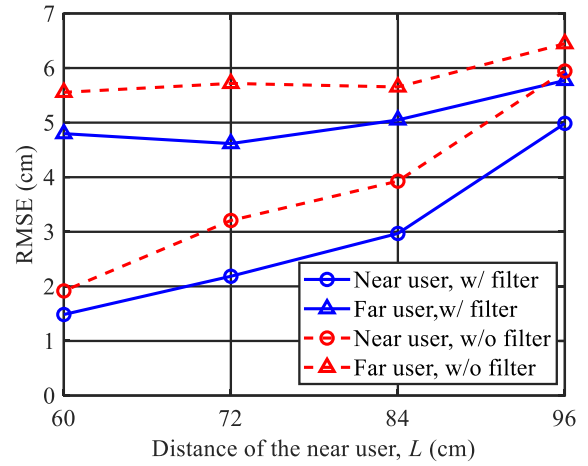


Fig. 5. Ranging RMSE vs. the distance of near user for different users without and with filter.

system, where the downlink Vpp is set to 100 mV.

Fig. 3 shows the downlink communication bit error ratio (BER) versus the distance of near user L for different users. For this figure, the vertical distance d between near user and far user is 10 cm, 20 cm and 30 cm respectively. As we can see, the BER is gradually increased with the increase of L for near and far users. The uplink communication BER versus the distance of near user L for different users without and with filter is shown in Fig. 4. The use of optical filter can substantially improve the uplink BER performance since bidirectional interference can be efficiently canceled via optical filtering. For the case without optical filtering, it is interesting to observe that the BER is close to 0.5 from 60 to 96 cm, which might be because the LD power is much greater than LED. Besides, for the case with optical filtering, it is observed that near user has a higher BER than far user. When applying conventional DFT-S-OFDM in practical bandlimited multi-user VLC systems, the low-pass frequency response of the system might cause unfairness among different user, since the near user occupying a higher-frequency subcarrier block suffers from a more severe power attenuation than that occupying a lower-frequency subcarrier block. More specifically, the maximum distances of near user for DFT-S-OFDM using 4-QAM to reach the 7% forward error correction (FEC) coding limit of 3.8×10^{-3} are about 84 cm.

Fig. 5 depicts ranging RMSE versus the distance of near user L for different user. For this figure, the far user is fixed at the distance of 96 cm and the time-domain window is 2560. As we can see, with the increase of L the ranging RMSE of the far and near user are both increased. Since the SNR received by near users is higher than that by far users, near users have better ranging performance. In addition, the use of optical filter can substantially improve ranging performance since the bidirectional interference can be efficiently canceled via optical filtering. For users at a greater distance, we should perform interference cancellation to remove the signals from closer users before conducting ranging for the farther users. Consequently, the ranging errors of closer users will affect the ranging performance of farther users. If the delay estimation for a closer user deviates from the correct value, the estimated signal of that closer user will be removed from an incorrect position during the interference cancellation process, which in turn leads to a degradation in interference cancellation performance.

IV. CONCLUSION

In this paper, we have firstly proposed and experimentally demonstrated a multi-user full-duplex RO-ISAC system. By using red and green lights with corresponding red and green optical filters, bidirectional interference can be mitigated and WDD-based full-duplex transmission can be established in the RO-ISAC system. To range the distances of multi-user and cancel the interference between the reflected signals, we have further proposed an interference cancellation scheme for the multi-user full-duplex RO-ISAC system. Experimental results successfully verify the feasibility of the proposed WDD-based multi-user full-duplex RO-ISAC system.

REFERENCES

- [1] F. Liu, Y. Cui, C. Masouros, J. Xu, T. X. Han, Y. C. Eldar, and S. Buzzi, "Integrated sensing and communications: Toward dual-functional wire-less networks for 6G and beyond," *IEEE J. Sel. Areas Commun.*, vol. 40, no. 6, pp. 1728–1767, 2022.
- [2] N. Gonzalez-Prelcic, M. F. Keskin, O. Kaltiokallio, M. Valkama, D. Dardari, X. Shen, Y. Shen, M. Bayraktar, and H. Wymeersch, "The integrated sensing and communication revolution for 6G: Vision, techniques, and applications," *Proc. IEEE*, vol. 112, no. 7, pp. 676–723, 2024.
- [3] Y. Wen, F. Yang, J. Song, and Z. Han, "Optical integrated sensing and communication: Architectures, potentials and challenges," *IEEE Internet Things Mag.*, vol. 7, no. 4, pp. 68–74, 2024.
- [4] Y. Cui, C. Chen, Y. Cai, Z. Zeng, M. Liu, J. Ye, S. Shao, and H. Haas, "Retroreflective optical ISAC using OFDM: Channel modeling and performance analysis," *Opt. Lett.*, vol. 49, no. 15, pp. 4214–4217, 2024.
- [5] H. Wang, Z. Zeng, C. Chen, B. Zhu, S. Shao, and M. Liu, "Retroreflective optical ISAC supporting 3D positioning in indoor environments," in *Proc. Asia Commun. Photon. Conf. (ACP)*, 2024, pp. 1–5.
- [6] S. Shao, A. Salustri, A. Khreishah, C. Xu, and S. Ma, "R-VLCP: Channel modeling and simulation in retroreflective visible light communication and positioning systems," *IEEE Internet Things J.*, vol. 10, no. 13, pp. 11 429–11 439, 2023.
- [7] H. Wang, C. Chen, Z. Zeng, S. Shao, and H. Haas, "Bidirectional retroreflective optical ISAC using time division duplexing and clipped OFDM," *IEEE Photon. Technol. Lett.*, 2025.
- [8] S. H. Chen, C. Chen, Z. H. Zeng, Y. B. Yang, and H. Haas, "Full-duplex RO-ISAC system: Wavelength division duplexing and hybrid waveform design," *IEEE Photon. Technol. Lett.*, vol. 37, no. 15, pp. 869–872, Aug. 2025.
- [9] T. T. Chu, J. Ye, C. Chen, X. Y. Guo, Z. H. Zeng, S. S. Guo, H. Haas, and M.-S. Alouini, "Revolutionizing 6G: Experimental validation of an optical integrated communication, sensing, and power transfer system," *IEEE J. Sel. Areas Commun.*, 2025.